Fundamental measure theory for pure systems with soft, spherically repulsive interactions

2002 J. Phys.: Condens. Matter 14 11921

(http://iopscience.iop.org/0953-8984/14/46/303)

INSTITUTE OF PHYSICS PUBLISHING JOURNAL OF PHYSICS: CONDENSED MATTER

J. Phys.: Condens. Matter **14** (2002) 11921–11932 PII: S0953-8984(02)37727-0

Fundamental measure theory for pure systems with soft, spherically repulsive interactions

M B Sweatman

Department of Chemistry, Imperial College of Science, Technology and Medicine, Exhibition Road, London SW7 2AY, UK

Received 6 June 2002, in final form 30 August 2002
Published 8 November 2002
Online at stacks.iop.org/JPhysCM/14/11921

Abstract

Fundamental measure theory (FMT) has recently been extended to penetrable spheres and soft spherical interactions (soft-FMT) (Schmidt M 1999 *Phys. Rev.* E **60** R6291; 2000 *J. Phys.: Condens. Matter* **11** 10 163). This paper presents these theories in a unified description for a pure system and also describes a simple procedure that is thought to improve the accuracy of FMT for soft, spherically repulsive interactions. An ultra-soft interaction, which is a model for the interaction of star polymers with arm number about 8 in a good solvent, is investigated and a simple procedure is found to significantly improve the accuracy of bulk thermodynamic and pair-correlation functions generated by soft-FMT when compared to Monte Carlo simulation results. The simple procedure also improves prediction of the bulk pressure–density relationship for a square-shoulder system. Similar gains in accuracy are expected for a wide range of soft interactions.

1. Introduction

Density functional theory (DFT) has played an important role in understanding how equilibrium properties of classical many-body systems are related to geometric properties of the individual particles. In some theories these geometric properties are described by weight functions that are central to the construction of the functional.

Nordholm and co-workers [1] introduced the first weighted DFT for a three-dimensional (3D) classical system. They considered the simplest non-trivial system, the mono-disperse hard-sphere system, and, inspired by Percus' exact solution for hard rods [2], employed the simplest weight function geometrically related to the pair interaction, i.e. the weight function is a hard-sphere Mayer function. In the twenty or so years since this innovation there has been considerable progress in the development and understanding of weighted-density functionals for a wide range of systems [3].

Tarazona [4] introduced a much more accurate hard-sphere functional, the 'smoothed density approximation' (SDA), by employing the 'semi-exact' Carnahan–Starling equation of

state for hard spheres [5] and introducing several weight functions fitted to reference 3D bulk fluid data. Recently, a similar approach has been employed for the Lennard-Jones fluid [6]. Despite the success of the SDA, this general approach suffers from two deficiencies. The most serious is that bulk fluid data is required as *input* to the theory. This presents a practical barrier for applications to fluids where this data is limited. The second is that confidence in the performance of the functional reduces as the degree of non-uniformity increases since such functionals take uniform fluid data as input. By depending on such data the functional loses sight of the 'fundamental' geometric properties of the particles.

Rosenfeld [7] and Kierlik and Rosinberg [8] developed the first fundamental measure theory (FMT) for hard spheres, the fundamental measure functional (called FMF1 in this paper). The only input required in Rosenfeld's approach is the form of the pair interaction. This leads automatically to the definition of a set of weight functions that deconvolute the Mayer function, and so are geometrically related to the pair interaction. The weight functions, together with an equation of state for the non-uniform hard-sphere system, reproduce as *output* Percus–Yevick (PY) thermodynamics and pair correlations for a 3D bulk fluid [5]. In addition, Rosenfeld showed [9] that this procedure can be performed in lower dimensions and that it is exact in one and zero dimensions, i.e. for hard rods and a density dot. As expected, the 3D functional (FMF1) is very accurate for more general applications such as a hard sphere fluid confined by a hard wall [8]. Rosenfeld also showed [10] that FMT can be applied to hard spheroids-of-revolution by application of the Gauss–Bonnet theorem.

By employing the same arguments used by Rosenfeld to derive FMF1 Cuesta and Martinez-Raton [11] constructed a fundamental measure functional (FMF) for the 'toy model' of parallel hard cubes. In this system the angular orientation of each cube is identical and held fixed so that interactions occur by 'slapping' cube faces.

More recently an alternative route to FMT for hard spheres has been discovered [12–15]. The key to this route is 'dimensional crossover' whereby a form of the FMF is sought such that it remains accurate for density distributions with reduced dimensionality. That is, accuracy is sought for the 3D functional when applied to hard disks, rods and density dots. Clearly, the exact hard-sphere functional possesses exact dimensional crossover behaviour. 'Theoretical interpolation' suggests that a functional that is accurate for uniform densities *and* extremely non-uniform densities will probably be accurate for intermediate non-uniformities. The motivation for this approach resulted from analysis of the performance of the original functional, FMF1 [9, 12]. It was found that the 3D functional was deficient since it produced divergent terms for hard rods and it could not 'stabilize' an array of 'density-Gaussians' (modelling the solid phase), i.e. the grand potential of such a distribution was always higher than that of the uniform fluid with corresponding average density. In quick succession [12, 13], several different functional forms of the hard-sphere FMF were proposed (including a functional called FMF2 in this paper, which is described later) with improved dimensional crossover behaviour, including stabilization of the hard-sphere solid. Crucially, it was realized [14] that FMFs could be generated systematically by considering only the geometry of particles and properties of distributions of density dots. The most sophisticated of these functionals for hard spheres is due to Tarazona [15]. His functional, called FMF3 in this paper, is constructed to be exact for any distribution of three density dots. However, for thermodynamic and pair-correlation properties of the uniform 3D hard-sphere fluid these functionals (FMF1, FMF2 and FMF3) yield the same PY functions. So, finally, FMT avoids the two significant deficiencies of the SDA approach.

Schmidt has developed several important innovations for FMT. The first [16] concerns the general deconvolution of the Mayer function enabling creation of soft-FMFs, based on the fundamental geometric properties of soft particles, for a wide range of model interactions [17].

However, because the geometry (and weight functions) for a general soft interaction are different to those for hard spheres, soft-FMT is an extension of the FMT recipe rather than a complete extension of the theory to soft spheres. That is, soft-FMT yields only the exact thermodynamics for one density dot, not two or three as is the case for FMT3 applied to hard-sphere systems. So soft-FMT cannot be expected to be as accurate for general soft interactions as FMT3 is for hard spheres. A second innovation [18] concerns the application of dimensional crossover to spheres whose interaction is constant and finite whenever two spheres overlap, enabling creation of a FMF for penetrable spheres. Because the geometry of hard and penetrable spheres is identical, FMT3 is equally valid for hard and penetrable spheres.

These ideas are important because they allow construction of density functionals, based only on geometric properties of the particles and their behaviour in the zero-dimensional (0D) limit, for soft-matter systems that have received much attention recently, including polymers and colloidal suspensions. For example, soft-FMT been extended to 'additive' mixtures [19] and applied to a 'non-additive' model colloid–polymer mixture [20].

The purpose of this paper is to show that the hard, penetrable and soft-sphere FMFs can be unified into a single description for a pure system, and to present a simple procedure that improves the accuracy of soft-FMT for a system of soft, spherically repulsive spheres. For pure systems of hard and penetrable spheres the resulting functionals are identical to those previously obtained [15, 18]. It is demonstrated that, for a model describing the interaction of star polymers with arm number about 8 in a good solvent [16, 21], this procedure does indeed improve soft-FMT [16, 17, 21] with respect to 3D bulk thermodynamics and pair correlations. The 3D bulk thermodynamic properties of a square-shoulder fluid are also investigated, and again the accuracy is improved. It is expected that improved accuracy will be seen for other soft interactions, and for soft systems with lower dimensionality. However, the procedure may lead to a reduction in accuracy when the 3D functional is applied to a single density dot, i.e. the 0D system.

2. Fundamental measure functional

2.1. Definition

Within soft-FMT the intrinsic excess Helmholtz free-energy functional is approximated as

$$F^{ex}(T,[\rho(\boldsymbol{r})]) = k_B T \int \mathrm{d}\boldsymbol{r}_1\, \Phi(\{n_\alpha(\boldsymbol{r_1}, T)\}) \tag{1}$$

where k_B and T are Boltzmann's constant and the temperature, and for a pure system the weighted densities (or fundamental measures), n_α, are given by [21]

$$n_\alpha(\boldsymbol{r_1}, T) = \int \mathrm{d}\boldsymbol{r_2}\, \rho(\boldsymbol{r_2}) w_\alpha(r_{12}, T) \tag{2}$$

where w_α are density-independent weight functions and $r_{12} = |\boldsymbol{r}_1 - \boldsymbol{r}_2|$. The subscript α labels the type of weighted density and weight function, and can either be scalar (w_α, n_α), vectorial ($\boldsymbol{w}_\alpha$, $\boldsymbol{n}_\alpha$) or tensorial ($\hat{\boldsymbol{w}}_\alpha$, $\hat{\boldsymbol{n}}_\alpha$). The excess free energy density, Φ, is given by [21]

$$\begin{aligned}
\Phi &= \Phi_1 + \Phi_2 + \Phi_3 \\
\Phi_1 &= n_0 \mu_{0D} \\
\Phi_2 &= (n_1 n_2 - \boldsymbol{n}_{v1} \cdot \boldsymbol{n}_{v2}) \mu'_{0D} \\
\Phi_3 &= (\boldsymbol{n}_{v2} \cdot \hat{\boldsymbol{n}}_{t2} \cdot \boldsymbol{n}_{v2} - n_2 \boldsymbol{n}_{v2} \cdot \boldsymbol{n}_{v2} - \mathrm{tr}(\hat{\boldsymbol{n}}_{t2}^3) + n_2\, \mathrm{tr}(\hat{\boldsymbol{n}}_{t2}^2)) \mu''_{0D}/(16\pi/3)
\end{aligned} \tag{3}$$

where $k_B T \mu_{0D}$ is the excess chemical potential in a 0D cavity, tr denotes the trace and a dash denotes the partial derivative with respect to n_3. This is the general expression for Tarazona's FMF3 [15], except that the form of μ_{0D} remains to be specified.

2.2. Low-density limit

The weight functions are determined so that the low-density limit of the pair-direct correlation function, $c^{(2)}(r)$, is exact;

$$c^{(2)}(r;\rho=0)=f(r)=\exp(-\phi(r)/k_BT)-1=-2\mu'_{0D}(w_{03}(r)+w_{12}(r)-w_{v1v2}(r)) \quad (4)$$

where $f(r)$ is the Mayer function corresponding to the pair potential ϕ, and w_{ab} indicates the convolution $w_\alpha \otimes w_\beta$ with implied scalar product. This requirement forms the low-density limit of the theoretical interpolation. Clearly, the weight functions must deconvolute a function linearly related to the Mayer function.

Schmidt showed [17] that the weight functions that deconvolute the negative of the Mayer function are given by

$$\begin{aligned}
&\tilde{w}_2(k)=\pm\sqrt{\mathrm{i}k\tilde{f}(k)}\\
&w_2(r)=-\partial w_3(r)/\partial r\\
&\boldsymbol{w}_{v2}(r)=w_2(r)\boldsymbol{r}/r\\
&w_1(r)=w_2(r)/4\pi r\\
&\boldsymbol{w}_{v1}(r)=w_1(r)\boldsymbol{r}/r\\
&w_0(r)=w_1(r)/r
\end{aligned} \quad (5)$$

where the tilde denotes a one-dimensional Fourier transform:

$$\tilde{f}(k)=\int_{-\infty}^{\infty}\mathrm{d}r f(r)\exp(\mathrm{i}kr). \quad (6)$$

So for hard and penetrable spheres of radius R, w_2 becomes

$$w_2(r)=\delta(R-r)\sqrt{\frac{1-\exp(-V/k_BT)}{\mu'_{0D}(\rho=0)}} \quad (7)$$

where V is the value of ϕ when two spheres are closer than $2R$. More generally [17], for any spherically repulsive interaction

$$w_3(r=0)=\sqrt{\frac{1-\exp(-\phi(r=0)/k_BT)}{\mu'_{0D}(\rho=0)}}. \quad (8)$$

Finally, the tensorial weight function is formed by the dyadic product of a vector density and a unit spatial vector [17, 21];

$$\hat{\boldsymbol{w}}_{t2}(r)=\boldsymbol{w}_{v2}(r)\boldsymbol{r}/r. \quad (9)$$

Properties of the uniform fluid follow immediately. The excess Helmholtz free-energy density, f^{ex}, is

$$\frac{f^{ex}(\rho_b)}{k_BT}=n_0\mu_{0D}+n_1n_2\mu'_{0D}+n_2^3\mu''_{0D}/24\pi \quad (10)$$

and the pair-direct correlation function is

$$\begin{aligned}
c^{(2)}(r_{12};\rho_b)\equiv&-\left(\frac{\delta^2F^{ex}}{k_BT\delta\rho(\boldsymbol{r}_1)\delta\rho(\boldsymbol{r}_2)}\right)_{\rho_b}\\
=&\,2(\mu'_{0D}w_{03}(r_{12})+n_2\mu''_{0D}w_{13}(r_{12})+(n_1\mu''_{0D}+n_2^2\mu'''_{0D}/8\pi)w_{23}(r_{12}))\\
&+(n_0\mu''_{0D}+n_1n_2\mu'''_{0D}+n_2^3\mu''''/24\pi)w_{33}(r_{12})\\
&+2\mu'_{0D}(w_{12}(r_{12})-w_{v1v2}(r_{12}))+n_2\mu''_{0D}(w_{22}(r_{12})-w_{v2v2}(r_{12}))/4\pi
\end{aligned} \quad (11)$$

where ρ_b is a uniform (bulk) density.

2.3. Zero-dimensional limit

Soft-FMT is fully specified by $\mu_{0D}(n_3)$. The soft-FMT [16] defines $k_BT\mu_{0D}$ to be the excess chemical potential when particles are confined in a cavity such that all particle centres coincide. This situation corresponds to a density dot or the 0D limit and it forms the second interpolation state of soft-FMT.

Following [18], the excess chemical potential in the 0D limit is given exactly by

$$k_BT\mu_{0D} = k_BT(\mu_{0D}^{tot} - \mu_{0D}^{id}) = k_BT\ln(V_{0D}z/\bar{N}) \tag{12}$$

where $k_BT\mu_{0D}^{tot}$ is the total 0D chemical potential, $z = \exp(\mu_{0D}^{tot})$ is the fugacity and $\bar{N}$ is the average number of particles in V_{0D}. In the grand canonical ensemble the partition function is given by

$$\Xi = \sum_{N=0}^{\infty} \int \mathrm{d}\boldsymbol{r}_N \frac{z^N}{N!} \exp(-V_N/k_BT) \tag{13}$$

where $\mathrm{d}\boldsymbol{r}_N$ indicates the product of N spatial integrals and V_N is the total potential of a configuration of N particles. The average occupation number, $\bar{N}$, is given by

$$\bar{N} = -\partial\ln(\Xi)/\partial\mu_{0D}^{tot} = \frac{z\partial\Xi}{\Xi\partial z}. \tag{14}$$

The 0D grand partition function is

$$\Xi = \sum_{N=0}^{\infty} (V_{0D}z)^N b^{N(N-1)/2}/N! \tag{15}$$

where $b = \exp(-\phi(r=0)/k_BT)$. So, given $\bar{N}$, these relations can be inverted to obtain $V_{0D}z(\bar{N})$ and hence $\mu_{0D}(\bar{N})$. Finally, the value of n_3 at the centre of the cavity is related to $\bar{N}$ to obtain $\mu_{0D}(n_3)$ and this expression is also used for general density distributions. In the low-density limit, $\bar{N} \to 0$, it follows that $\mu'_{0D} \to (1-b)\partial\bar{N}/\partial n_3$. So for any spherically repulsive interaction a mutually consistent definition of the soft-FMF is obtained when $w_3(r=0) = 1$, and this constraint generates a unique set of weight functions for each interaction.

The above relations, (1)–(3), (5), (6), (9), (12), (14) and (15) fully define FMT in a unified description for pure systems of soft, penetrable and hard spheres. It yields the exact pair-correlation and thermodynamic functions for a uniform 3D fluid in the low-density limit and is also exact in the 0D limit. By construction, it is exact for hard and penetrable spheres for any 3D distribution of three density dots, but for other soft interactions it is exact for one density dot only. This is because FMF3 is derived for the unique geometry of hard and penetrable spheres only. Earlier versions of FMT [7, 13] have different forms for Φ_3:

$$\begin{aligned} &\text{FMF1}: \quad \Phi_3 = (n_2^3 - 3n_2\boldsymbol{n}_{v2}\cdot\boldsymbol{n}_{v2})\mu''_{0D}/24\pi \\ &\text{FMF2}: \quad \Phi_3 = n_2^3(1-(\boldsymbol{n}_{v2}/n_2)^2)^3\mu''_{0D}/24\pi \end{aligned} \tag{16}$$

that generate different functionals. Each of these functionals (FMF1, FMF2 and FMF3) yields the same 3D bulk thermodynamics (10) and pair correlation functions (11).

For interactions with $b = 0$, i.e. that are infinite at the origin, we have

$$\mu_{0D} = -\ln(1-n_3) \tag{17}$$

and so for these interactions the thermodynamics of the system are distinguished only by the form of w_3. Also, whatever the form of w_3, the functional predicts a finite upper limit for n_3 and hence for the bulk density of a given phase. However, for interactions that give $b \neq 0$, i.e. that are finite at the origin, we find that μ_{0D} is rather more complex and, whatever the form of w_3, the functional predicts that n_3 does not have a finite upper limit.

It is easy to imagine pair interactions for which these properties are inappropriate. For example, the square-shoulder potential defined by the pair interaction

$$\phi(r) = \begin{cases} \infty; & r \leqslant r_s \\ \phi_s; & r_s < r \leqslant \sigma \\ 0; & r > \sigma \end{cases} \tag{18}$$

is incorrectly predicted to have an upper limit $n_3 = 1$ for all values of r_s and ϕ_s. If ϕ_s/k_BT is large then the upper limit for n_3 should be close to $(\sigma/r_s)^3$. Similarly, any interaction that diverges at the origin, such as the interaction that models star polymers in good solution [17], is erroneously predicted to have a finite upper limit for n_3. In fact, the predicted high-density limit for these systems is inappropriate with respect to any dimensionality except zero. For example, FMF3 for star polymers has the same incorrect finite upper limit for n_3 when the functional is applied to star polymers confined in one and two dimensions.

However, for penetrable spheres

$$\phi(r) = \begin{cases} \phi_s; & 0 \leqslant r \leqslant \sigma \\ 0; & r > \sigma \end{cases} \tag{19}$$

and hard spheres ($\phi_s = \infty$) FMF3 has appropriate high-density limit behaviour, i.e. $n_3 < 1$ for hard spheres and n_3 has no upper limit for penetrable spheres. The error in predicting high-density behaviour within FMF3 for more general interactions arises because the high-density limit of a bulk 3D phase is dictated by μ_{0D} and hence $\phi(r = 0)$, while the form of ϕ for $r > 0$ only enters into the thermodynamics through the weight functions. But for hard and penetrable spheres $\phi(r \leqslant \sigma)$ is constant and so $\phi(r = 0)$ is representative of the interaction for all $r \leqslant \sigma$.

2.4. σ-cavity limit

This paper proposes an alternative prescription for the unified FMT for pure systems. Rather than attempting to construct a version of FMT for a general soft interaction that is exact for any distribution of three density dots (a daunting task), it is instead proposed that, for a 3D system, FMT3 and the definition of the soft weight functions are retained and an alternative prescription for μ_{0D} is found. Nevertheless, a prescription for μ_{0D} is sought that reproduces the correct expression for hard and penetrable spheres, since FMT3 is derived explicitly and is accurate, for this unique geometry. The aim is to include within μ_{0D} the effect of ϕ for $r \leqslant \sigma$ on the thermodynamics in an approximate manner, i.e. to generate a 'soft-μ_{0D}'. With this in mind, attention is drawn to the fact that, for hard and penetrable spheres, the excess chemical potential of such systems is identical when confined such that (a) particle centres coincide and (b) all pairs of particles overlap. The first case corresponds to the 0D limit and the excess chemical potential is $k_BT\mu_{0D}$. In this paper the second case is called the σ-cavity limit and has excess chemical potential equal to $k_BT\mu_{\sigma C}$. So, for spherically repulsive interactions with finite range σ, the σ-cavity is a sphere for a 3D system with diameter σ. For hard and penetrable spheres the equality, $\mu_{\sigma C} \equiv \mu_{0D}$, holds.

This paper proposes that soft-FMT be re-written with $\mu_{\sigma C}$ replacing μ_{0D}. The grand-partition function can be re-written exactly as

$$\Xi = \sum_{N=0}^{\infty} (V_{\sigma C} z)^N b_N^{N(N-1)/2} / N! \tag{20}$$

where $V_{\sigma C}$ is the volume of the σ-cavity and b_N is a series of coefficients. For $N = 0$, 1, 2 and a 3D system, these coefficients can be calculated exactly:

$$\begin{aligned} b_0 &= 1 \\ b_1 &= 1 \\ b_2 &= \frac{4\pi}{V_{\sigma C}} \int_0^{\sigma/2} \mathrm{d}r_1\, r_1^2 \bar{b}(r_1) \end{aligned} \tag{21}$$

where

$$\bar{b}(r_1) = \frac{\pi}{V_{\sigma C}} \left\{ 4 \int_0^{\sigma/2-r_1} \mathrm{d}r_2\, r_2^2 b(r_2) + \int_{\sigma/2-r_1}^{\sigma/2+r_1} \mathrm{d}r_2\, r_2 b(r_2)(\sigma^2/4 - (r_1 - r_2)^2)/r_1 \right\} \tag{22}$$

and now $b(r) = \exp(-\phi(r)/k_B T)$. Clearly, for hard and penetrable spheres $b_N = b(r = 0)$ for all N. But for more general interactions, for $N > 2$, it becomes increasingly difficult to determine b_N as N increases. This paper sets $b_N = 0$ for $N > 2$. Then $\mu_{\sigma C}(\bar{N})$ is analytic and given by [18]

$$\mu_{\sigma C} = k_B T \ln\left(\frac{\sqrt{(\bar{N}-1)^2 + 2\bar{N}(2-\bar{N})b_2} + \bar{N} - 1}{b_2(2-\bar{N})\bar{N}} \right) \tag{23}$$

and in the low-density limit $\mu'_{\sigma C}(n_3) \to (1-b)\partial\bar{N}/\partial n_3$. For penetrable spheres this result is identical to that obtained by Schmidt [18]. For hard spheres, $b_2 = 0$ and the functional reduces to that obtained by Tarazona [15]. For more general soft interactions the correct result for hard and penetrable spheres, $\partial\bar{N}/\partial n_3 = 1$, is enforced for all interactions.

3. Results

The accuracy of the 0D and σ-cavity soft-FMT approaches is compared for two model pair potentials at the level of pair functions and thermodynamics for bulk 3D fluids. This is equivalent to comparing the first three (the zeroth, first and second) coefficients generated by a density expansion (a functional Taylor series expansion about a bulk density) of the free-energy functional of each theory [20], and gives an indication of the accuracy of each theory when applied to the inhomogeneous fluid. Further detail could be obtained by comparing their dimensional crossover properties.

3.1. Star-polymer fluid; $q = 3$

A star polymer [23] consists of polymer chains of equal length that are joined at a central 'node'. Within soft-FMT the interaction between two star polymers in a good solvent has been modelled by [16]

$$w_3(r) = \begin{cases} 1 - x^q; & x \leqslant 1 \\ 0; & x > 1 \end{cases} \tag{24}$$

where q controls the softness of the interaction and $x = 2r/\sigma$. The value $q = 3$ models star polymers with about 8 'arms', an ultra-soft system. Using the definitions for the soft weight functions (7), this yields an effective pair potential

$$\phi_{*3}/k_B T = \begin{cases} -\ln(0.05x^6); & x \leqslant 1 \\ -\ln(-0.05x^6 + 2x^3 - 4.5x^2 + 3.6x - 1); & 1 < x \leqslant 2 \\ 0; & x > 2. \end{cases} \tag{25}$$

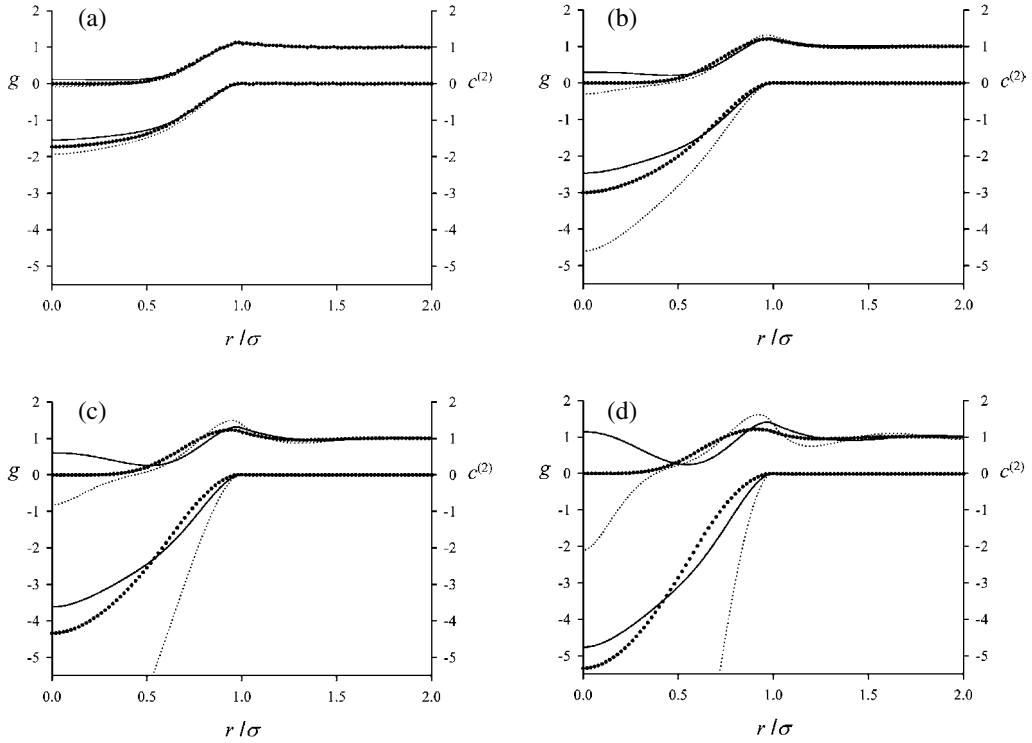

Figure 1. (a) Radial distribution function, $g(r)$, and pair-direct correlation function, $c^{(2)}(r)$, for a model star-polymer fluid with $q = 3$ (see text) at a reduced bulk density, $\rho\sigma^3 = 0.402$. The small circles, full curves and dotted curves correspond to results from GCEMC simulation, σ-cavity and 0D soft-FMFs, respectively (see text). r is the radial distance and σ is the length scale of the star-polymer interaction. (b) As for (a) except that $\rho\sigma^3 = 0.889$. (c) As for (a) except that $\rho\sigma^3 = 1.366$. For the 0D FMF approach, $c^{(2)}(r = 0) = -11.9$. (d) As for (a) except that $\rho\sigma^3 = 1.818$. For the 0D FMF approach, $c^{(2)}(r = 0) = -32.8$.

This in turn yields $b_2 = 0.21$ from (21) and (22). Results for pair-correlation functions and excess pressure of a bulk 3D fluid of star polymers with $q = 3$ are shown in figures 1(a), (b), (c), (d) and 2(a), respectively. In each case the pair-direct correlation function, $c^{(2)}(r)$, is obtained from (11), i.e. directly from the FMFs. The corresponding pair-distribution functions, $g(r)$, are obtained from each $c^{(2)}(r)$ by application of the Ornstein–Zernike relation [5]. The corresponding excess pressures, shown in figure 2(a), are obtained from the respective FMF by

$$P^{ex} = k_B T \rho^2 \left(\frac{\partial(\Phi/\rho)}{\partial\rho} \right)_{T,V}. \tag{26}$$

Clearly, this will *not* correspond to the excess pressure of the real system of star polymer plus solvent, but the comparison in figure 2(a) is useful as a comparison of the accuracy of the respective theories. The theories are compared with grand-canonical ensemble Monte Carlo (GCEMC) simulation results.

The simulation parameters and results for pressure and density are given in table 1. The simulation pair-direct correlation functions, $c^{(2)}(r)$, shown in figures 1(a)–(d) are obtained from the simulation pair-distribution functions, $g(r) = h(r) + 1$, and the Ornstein–Zernike relation [5]. In each case $g(r)$ for $r > L/2$ is set to 1, where L is the simulation box

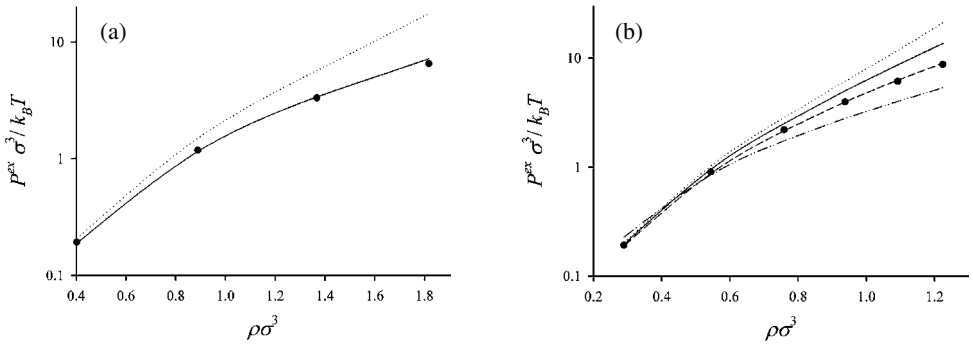

Figure 2. (a) Reduced excess pressure (see text) for a model star-polymer fluid with $q = 3$ (see text) for a range of bulk densities. The small circles, full curve and dotted curve correspond to results from GCEMC simulation, σ-cavity and 0D soft-FMF approaches, respectively. The reduced excess pressure is drawn on a logarithmic scale. Statistical errors from simulation are always less than the size of the large dots at the level of 1 s.d. (b) Reduced excess pressure (see text) for a model square-shoulder fluid with $(r_s/\sigma)^3 = 0.5$ and $\phi_s/k_BT = 1.0$ (see equation (18)) for a range of bulk densities. The small circles, full curve, dotted curve, broken curve and chain curve correspond to results from GCEMC simulation, σ-cavity ($b_2 = 0.04$) soft-FMT, 0D soft-FMT, σ-cavity ($b_2 = 0.1$) soft-FMT and mean-field (see equation (28)) approaches, respectively. The reduced excess pressure is drawn on a logarithmic scale. Statistical errors from simulation are always less than the size of the large dots at the level of 1 s.d.

Table 1. GCEMC simulation parameters and results for systems modelling star polymers in good solution with $q = 3$ (see text). $z = \exp(\beta\mu)$ is the activity, N_{run} and N_{eqm} are the number of attempted Monte Carlo moves used to gather statistics and to achieve equilibrium respectively. L is the simulation box length, ρ is the density and P^{ex} is the excess (over ideal gas) pressure. The numbers in parentheses indicate the standard deviation in the last significant figure.

$z^* = z\sigma^3$	N_{run} (10^6)	N_{eqm} (10^6)	$L^* = L/\sigma$	$\rho^* = \rho\sigma^3$	$P^{ex*} = P^{ex}\sigma^3/k_BT$
1	10	1	6	0.4020(4)	0.189(1)
10	10	1	6	0.8893(6)	1.174(3)
100	10	1	8	1.3657(7)	3.295(5)
1000	10	1	8	1.8180(6)	6.509(6)

length. Various values of the box length are chosen, with the final value for L chosen for each chemical potential such that there is no significant change in the simulation results (including pair-correlation functions) when it is increased by 2σ. A radial grid of 100 points per σ is chosen and fast Fourier transforms [24] are employed.

It can be seen that, for the bulk densities considered, the σ-cavity soft-FMT approach is generally closer to the simulation results than the 0D soft-FMT approach. In particular, for excess pressure the σ-cavity approach is quite accurate over the density range studied and is much more accurate than the 0D approach. The 0D functional is accurate at low to moderate densities, but loses accuracy as the bulk density is increased beyond this regime. However, the σ-cavity functional remains accurate up to reasonably high densities, and loses accuracy as the average separation of particles decreases below σ. Note that DFT does not automatically constrain $g(r)$ obtained via the Ornstein–Zernike relation from $c^{(2)}(r)$ obtained directly from functional differentiation of the theory. So the unphysical values of $g(r)$ for $r/\sigma \leqslant 0.5$ are of little concern and can be corrected by finding solutions in the test-particle limit.

Table 2. GCEMC simulation parameters and results for the square-shoulder potential (see equation (18)) with $(r_s/\sigma)^3 = 0.5$ and $\phi_s/k_BT = 1.0$. The meaning of the column headings and numbers in parentheses is the same as for table 1.

z^*	N_{run} (10^6)	N_{eqm} (10^6)	L^*	ρ^*	P^{ex*}
1	5	1	4	0.2883(8)	0.187(7)
10	5	1	4	0.5430(8)	0.90(1)
100	5	1	4	0.7583(8)	2.16(4)
1 000	5	1	4	0.937(1)	3.99(7)
10 000	5	1	4	1.088(2)	6.1(2)
100 000	5	1	4	1.224(4)	8.7(2)

3.2. A square-shoulder fluid

The square-shoulder pair potential (18) has previously been employed to model liquid metals, but it could also form the reference potential of a perturbation theory of water (see [25] and references therein). In the latter case the square-shoulder models the resistance to the breaking of hydrogen bonds as water is compressed to high pressure. Despite these important applications, the square-shoulder system has not previously been analysed within soft-FMT. Figure 2(b) shows the prediction of excess pressure by the 0D and σ-cavity ($b_2 = 0.04$) soft-FMT approaches compared with GCEMC simulation results for a square-shoulder system with $(r_s/\sigma)^3 = 0.5$ and $\phi_s/k_BT = 1$. The GCEMC simulation parameters and results are given in table 2. The excess pressure is calculated from the simulated $g(r)$ using [5]

$$\frac{P^{ex}}{k_BT} = \frac{2\pi}{3}\rho^2(g(r_s)r_s^3 + g(\sigma)\sigma^3(1 - \exp(-\phi_s/k_BT))). \tag{27}$$

Once again, various values of the box length are chosen, with the final value for L chosen for each chemical potential such that there is no significant change in the simulated pressure or density when it is increased by 2σ.

The soft-FMT results are obtained by making use of the relations in [17] equating moments of the Mayer function with the 'volumes', ξ_α, of the soft-FMT weight functions. For the σ-cavity functional, the correct volumes are obtained by dividing each ξ_α by $(1 - b_2)^{1/2}$. These relations allow calculation of the bulk equation of state from the pair potential, together with (4), without explicit calculation of weight functions. Also shown in figure 2(b) are the results obtained from the σ-cavity approach with $b_2 = 0.1$ and a simple mean-field DFT, with the excess pressure given by

$$P^{ex} = P^{ex}_{HS}(\rho/2) + 2\pi\phi_s\rho^2/3 \tag{28}$$

for this square-shoulder fluid, where P^{ex}_{HS} is the excess pressure of the reference hard-sphere system (using the PY equation of state for hard spheres). This type of theory is commonplace in the DFT literature [3], particularly when treating the Lennard-Jones fluid. Once again, the σ-cavity soft-FMT approach ($b_2 = 0.04$) yields results that are closer to simulation than the 0D approach. However, the agreement is not as good for this system as for the star polymer system with $q = 3$ above. However, choosing $b_2 = 0.1$ provides a good fit to the simulation data. The simple mean-field theory generally performs as well as the σ-cavity functional, and better than the 0D functional, for the excess pressure at high densities, but is poor at low densities.

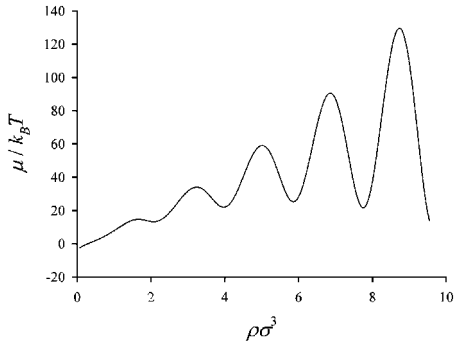

Figure 3. Reduced chemical potential, μ/k_BT, for a model penetrable sphere fluid with $\phi_s/k_BT = 2.0$ (see equation (19)) for a range of bulk densities predicted by the σ-cavity and 0D soft-FMTs. Note the oscillatory regime for $\rho\sigma^3 > 1.5$.

4. Conclusions

Soft-FMT has been unified with the hard and penetrable-sphere FMFs for pure systems. The performance of the unified approach, called the '0D' functional in this paper, has been improved, at least for the systems considered here. The improved approach, that uses the 'σ-cavity' functional, can be applied to a wide range of spherically repulsive pair potentials. However, its accuracy regarding pair potentials with significant attractive forces, such as the Lennard-Jones potential, has not been assessed.

Similar improvements in accuracy are expected for most other density distributions, including the 2D and 1D limits. That is, similar improvements are expected when the 3D theories are applied to 2D and 1D distributions. However, when the 3D theories are applied to 0D distributions (a single density dot) the original 0D theory will generally be more accurate since it is defined to be exact in this limit. Note, however, that 0D versions of the σ-cavity approach and the 0D approach are identical (since the σ-cavity corresponds to the 0D limit in this case). This observation leads one to speculate whether the correct dimensional crossover can be imposed on $\mu_{\sigma C}$. Perhaps a more fruitful task would be to attempt construction of a soft-FMF that is exact for at least two density dots for the square-shoulder pair potential with arbitrary r_s and ϕ_s. If successful, the insight gained might lead to the creation of accurate FMFs for more general soft interactions.

For the star-polymer system studied here the σ-cavity functional is probably limited in utility to $n_3 < 0.5$. It is possible that the use of density-dependent weight functions might improve performance in this respect. Schmidt has suggested such an approach based on the Wigner–Seitz radius [16, 17]. Alternatively, for high-density systems an SDA-type functional could be used [6]. But, as mentioned in the introduction, this approach suffers from two major deficiencies, namely that reference pair-correlation and thermodynamic data for the uniform fluid is required as input, and the functional cannot be expected to be accurate for extreme inhomogeneities.

The σ-cavity functional can be tuned to fit reference data, if required, by adjusting the values of b_N. For example, choosing $b_2 = 0.1$ provides a good fit to the excess pressure for the above square-shoulder system over the density range studied here. However, a feature of the σ-cavity functional and the 0D functional for penetrable spheres is that they can predict a series of first-order isotropic fluid–fluid transitions with increasing pressure, with the number of predicted transitions often increasing with the number of non-zero terms in the series, b_N.

This regime begins above the densities considered in this paper. This is illustrated in figure 3 which shows the reduced bulk chemical potential, μ/k_BT, predicted by the σ-cavity and 0D functionals for penetrable spheres with $\phi_s/k_BT = 2$ for a range of bulk densities up to $n_3 = 5$. Note how the oscillatory chemical potential regime in this example begins at bulk densities where the average separation of particles is somewhat less than σ, i.e. $\rho\sigma^3 > 1.5$. The σ-cavity functional can predict qualitatively similar behaviour for a wide range of soft fluids, depending on the values in the series b_N, when it is not expected. So it is unlikely that the σ-cavity functional can be fitted to reference data over a very wide range of densities.

It is not clear whether the unified 0D functional or the σ-cavity functional can be extended to mixtures. Schmidt has extended soft-FMT to mixtures [19] when the pair potential of each component is not finite at the origin. For more general interactions, a first step in this direction would be to consider a binary mixture of penetrable spheres with different r_s and ϕ_s.

References

[1] Nordholm S, Johnson M and Freasier B C 1980 *Aust. J. Chem.* **33** 2139
[2] Percus J K 1976 *J. Stat. Phys.* **15** 505
Percus J K 1982 *J. Stat. Phys.* **28** 67
[3] Evans R 1992 *Fundamentals of Inhomogeneous Fluids* ed D Henderson (New York: Wiley)
[4] Tarazona P 1985 *Phys. Rev.* A **31** 2672
Tarazona P 1985 *Phys. Rev.* A **32** 3148
[5] Hansen J P and McDonald I R 1986 *Theory of Simple Liquids* 2nd edn (London: Academic)
[6] Sweatman M B 2001 *Phys. Rev.* E **63** 031102
Sweatman M B 2002 *Phys. Rev.* E **65** 011102
[7] Rosenfeld Y 1989 *Phys. Rev. Lett.* **63** 980
Phan S, Kierlik E, Rosinberg M L, Bildstein B and Kahl G 1993 *Phys. Rev.* E **48** 618
[8] Kierlik E and Rosinberg M L 1990 *Phys. Rev.* A **42** 3382
[9] Rosenfeld Y 1993 *J. Chem. Phys.* **98** 8126
[10] Rosenfeld Y 1994 *Phys. Rev.* E **50** R3318
[11] Cuesta J A 1996 *Phys. Rev. Lett.* **76** 3742
Cuesta J A and Martinez-Raton Y 1997 *Phys. Rev. Lett.* **78** 3681
[12] Rosenfeld Y, Schmidt M, Löwen H and Tarazona P 1997 *Phys. Rev.* E **55** 4245
[13] Rosenfeld Y, Schmidt M, Löwen H and Tarazona P 1996 *J. Phys.: Condens. Matter* **8** L577
[14] Tarazona P and Rosenfeld Y 1997 *Phys. Rev.* E **55** R4873
[15] Tarazona P 2000 *Phys. Rev. Lett.* **84** 694
[16] Schmidt M 1999 *Phys. Rev.* E **60** R6291
[17] Schmidt M 2000 *Phys. Rev.* E **62** 4976
[18] Schmidt M 2000 *J. Phys.: Condens. Matter* **11** 10 163
[19] Schmidt M 2000 *Phys. Rev.* E **62** 3799
[20] Schmidt M, Lowen H, Brader J M and Evans R 2000 *Phys. Rev. Lett.* **85** 1934
[21] Groh B and Schmidt M 2001 *J. Chem. Phys.* **114** 5450
[22] Sweatman M B 2000 *Mol. Phys.* **98** 573
[23] Likos C N 2001 *Phys. Rep.* **348** 267
[24] Press W H, Teukolsky S A, Vetterling W T and Flannery B P 1992 *Numerical Recipes in Fortran 77: The Art of Scientific Computing* 2nd edn (Cambridge: Cambridge University Press)
[25] Franzese G, Malescio G, Skibinsky A, Buldyrev V and Stanley H E 2001 *Nature* **409** 692